

Computational angular oscillatory motion for a .50 caliber bullet type firing from a helicopter machine gun

Dimitrios N. Gkritzapis¹ and Elias E. Panagiotopoulos¹

Abstract

The present study investigates the epicyclic pitching and yawing motion phenomenon of spinning symmetric projectiles applying the 6-DOF free flight dynamic simulation modelling for small-yaw flat-fire trajectories. The computational results are compared with the corresponding classical second order linear differential solution. The ammunition will be used is the .50 API M8 bullet firing from M2 machine gun launched horizontally from different firing angles on high-speed subsonic aircraft (helicopter). This analysis includes mean constant coefficients of the most significant aerodynamic forces, moments and Magnus effects, which have been taken from official tabulated database.

Keywords: Bullet Projectile Type, Epicyclic Pitching and Yawing Motion, Trajectory Dynamics Simulation, Symmetric Projectiles, Subsonic Aircraft.

¹ Department of Mathematical and Engineering Sciences, Hellenic Military Academy, Vari, Attiki, 16673, Greece

1 Introduction

External ballistics (McShane et. al. 1953; McCoy 1999; Gkritzapis & Panagiotopoulos 2008) deals with the behavior of a non-powered projectile in flight. Many forces act upon the projectile during this phase including gravity, air resistance and air density.

Pioneering English ballisticians Fowler, Gallop, Lock & Richmond (1920) constructed the first rigid six-degree-of-freedom projectile exterior ballistic model. The trajectory deflection from the aircraft on a .30 caliber machine gun bullet was first addressed in 1943 by T. E. Sterne (1943). This reference was written from mathematicians who were tasked with generating firing tables for the machine guns, used sidewise fire from high speed airplanes.

The present work address the application of the full six degree of freedom (6-DOF) projectile flight dynamics modelling on the accurate trajectory prediction of high spin-stabilized bullets firing sidewise in different angles (30° , 60° and 90° test cases) from a high subsonic air vehicle. It takes into consideration the influence of the most significant forces and moments, based on appropriate constant mean values of the aerodynamic coefficients. The angular oscillatory motion with initial firing small yaw angles and flat-fire trajectory motions is compared with the corresponding classical second order linear differential solutions for high-spin spinning projectiles as the 12.95 mm M8 API bullet projectile type.

2. Projectile Model

The M8 API (armor piercing incendiary) was put into service in 1943 to replace the M1 Incendiary, and is still in service today. The M8 is built nearly identical to the M2 Armor Piercing except the M8 has 12 grains of incendiary mix in the nose instead of lead filler, and a lead caulking disc in the base acting as a

seal. Having the same hardened steel core as the M2, the M8 matches the armor piercing capability of the M2 with the added advantage of incendiary effect. While it has considerably less incendiary mix than the M1, the performance of the M8 was greatly superior to the M1 because of its ability to penetrate the target and ignite the material inside rather than just flash on the surface like the M1 often did, making for a greater first shot effect. Pyrotechnic performance of these projectiles is only slightly less than the M1 Incendiary. The present analysis considers the type of representative flight bullet vehicle.

Physical and geometric characteristics data of the above mentioned 12.95 mm M8 API bullet and Browning M2 .50 Caliber machine gun are illustrated in Table 1 and Figure 1, respectively.

Table 1: Physical and geometrical data of 12.95 mm API M8 bullet

Characteristics	API M8 Bullet
Reference diameter D , mm	12.95
Total length L , cal	4.46
Mass m , kg	0.0419
Center of gravity $x_{C.G.}$, cal	1.79 (from the base)
Axial moment of inertia, $\text{kg}\cdot\text{m}^2$	$0.7843\cdot 10^{-6}$
Transverse moment of inertia, $\text{kg}\cdot\text{m}^2$	$0.7389\cdot 10^{-5}$



Figure 1: .50 Caliber M8 API and Browning M2 .50 Caliber machine gun

3 Trajectory Flight Simulation Model

The projectile can be modelled as rigid body possessing six degrees-of-freedom (6-DOF) including three inertial position components x , y and z of the system mass center as well as the three Euler orientation angles φ , θ and ψ (see for example Amoruso 1996; Hainz & Costello 2005).

Two mean coordinate systems are used for the computational approach of the atmospheric flight motion. The one is a plane fixed (inertial frame, if) at the ground surface, which its center O_1 lies on the projection of the firing point on ground surface, as depicted in Figure 2. The other is a no-roll rotating coordinate system that is attached to, and moving with, the projectile's center of mass O_2 (no-roll-frame, NRF, $\varphi = 0$) with X_{NRF} axis along the projectile's axis of revolution positive from tail to nose (Figure 2). Y_{NRF} axis is perpendicular to X_{NRF} lying in the horizontally plane. Z_{NRF} axis oriented so as to complete a right-hand orthogonal system.

Newton's laws of motion state that rate of change in linear momentum must equal to the sum of all the externally applied forces and the rate of change in angular momentum must equal to the sum of all the externally applied moments, respectively. The force acting on the projectile comprises the weight, the aerodynamic forces and the Magnus force. On the other hand, the moment acting on the projectile comprises the moment due to the standard aerodynamic force, the Magnus aerodynamic moment and the unsteady aerodynamic moment.

The twelve state variables x , y , z , φ , θ , ψ , \hat{u} , \hat{v} , \hat{w} , \hat{p} , \hat{q} and \hat{r} are necessary to describe position, flight direction and velocity at every point of the projectile's atmospheric trajectory. Introducing the components of the acting forces and moments expressed in the no-roll-frame ($\hat{*}$) with the dimensionless arc length l expresses the projectile downrange travel in calibers, as an independent variable

$$I = \frac{I}{D} s = \frac{I}{D} \int_0^t V dt \quad (3.1)$$

the following modified linear equations of motion are derived (see Hainz & Costello 2005):

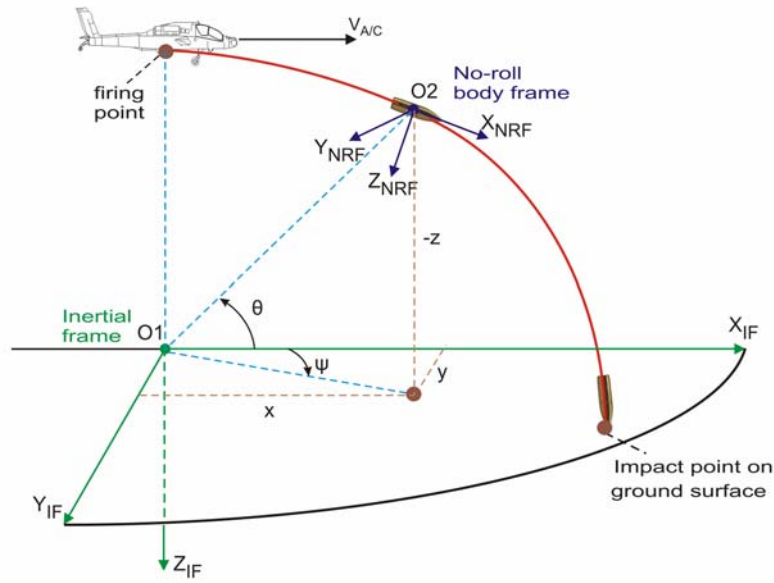


Figure 2: No-roll (moving) and fixed (inertial) coordinate systems for the atmospheric flight trajectory of flat-firing projectiles from a high-speed aircraft vehicle.

$$\frac{dx}{dl} = \frac{D}{V} (\cos \theta \hat{u} - \psi \hat{v} + \sin \theta \hat{w}) \quad (3.2)$$

$$\frac{dy}{dl} = \frac{D}{V} (\psi \cos \theta \hat{u} + \hat{v} + \psi \sin \theta \hat{w}) \quad (3.3)$$

$$\frac{dz}{dl} = \frac{D}{V} (-\sin \theta \hat{u} + \cos \theta \hat{w}) \quad (3.4)$$

$$\frac{d\varphi}{dl} = \frac{D}{V}(\hat{p} + \tan \theta \hat{r}) \quad (3.5)$$

$$\frac{d\theta}{dl} = \frac{D}{V} \hat{q} \quad (3.6)$$

$$\frac{d\psi}{dl} = \frac{D}{V \cos \theta} \hat{r} \quad (3.7)$$

$$\frac{d\hat{u}}{dl} = -\frac{D}{V} g \sin \theta - \frac{\rho S_{ref} D}{2m} C_D V \quad (3.8)$$

$$\frac{d\hat{v}}{dl} = -\frac{\rho S_{ref} D}{2m} (C_{LA} + C_D)(\hat{v} - \hat{v}_w) - D \hat{r} \quad (3.9)$$

$$\frac{d\hat{w}}{dl} = -\frac{\rho S_{ref} D}{2m} (C_{LA} + C_D)(\hat{w} - \hat{w}_w) + D \hat{q} + \frac{D}{V} g \cos \theta \quad (3.10)$$

$$\frac{d\hat{p}}{dl} = \frac{\pi \rho D^5}{16 I_{YY}} C_{RD} \hat{p} \quad (3.11)$$

$$\begin{aligned} \frac{d\hat{q}}{dl} = & \frac{\pi \rho D^4}{16 I_{YY} V} L_{CGCM} C_{MaM} \hat{p} (\hat{v} - \hat{v}_w) + \frac{\pi \rho D^3}{8 I_{YY}} L_{CGCP} (C_{LA} + C_D)(\hat{w} - \hat{w}_w) + \\ & + \frac{\pi \rho D^5}{16 I_{YY}} C_{PD} \hat{q} + \frac{\pi \rho D^4}{8 I_{YY}} C_{OM} - \frac{I_{XX}}{I_{YY}} \frac{D}{V} \hat{p} \hat{r} \end{aligned} \quad (3.12)$$

$$\begin{aligned} \frac{d\hat{r}}{dl} = & \frac{\pi \rho D^4}{16 I_{YY} V} L_{CGCM} C_{MaM} \hat{p} (\hat{w} - \hat{w}_w) - \frac{\pi \rho D^3}{8 I_{YY}} L_{CGCP} (C_{LA} + C_D)(\hat{v} - \hat{v}_w) + \\ & + \frac{\pi \rho D^5}{16 I_{YY}} C_{PD} \hat{r} - \frac{\pi \rho D^4}{8 I_{YY}} C_{OM} - \frac{I_{XX}}{I_{YY}} \frac{D}{V} \hat{p} \hat{q} \end{aligned} \quad (3.13)$$

Equations (3.2–3.13) form the modified linear theory equations of motion for a projectile and must be numerically integrated to estimate a trajectory. The following set of simplifications was employed for the previous flight dynamic model:

1) The station line velocity \hat{u} and roll rate \hat{p} are large in relation to the side velocities \hat{v} and \hat{w} , yaw angle ψ , pitch and yaw rates \hat{q} and \hat{r} , and wind velocity components \hat{v}_w and \hat{w}_w . Products of small values and derivatives of small values are treated as negligible.

2) The yaw angle ψ is small, allowing the simplifications

$$\sin\psi \approx \psi \quad \cos\psi \approx 1 \quad (3.14)$$

3) The aerodynamic angles of attack α and sideslip β remain small ($< 15^\circ$) for the main part of the atmospheric trajectory (see for example Hainz & Costello 2005):

$$\alpha \approx \frac{\hat{w} - \hat{w}_w}{V} \quad \beta \approx \frac{\hat{v} - \hat{v}_w}{V} \quad (3.15)$$

4) The Magnus force components are small in comparison with the weight and aerodynamic force components, and so they are treated as negligible in the modified linear theory computations. The Magnus force does create a non-negligible moment, and so it is maintained in the moment computations.

5) The projectile is geometrically symmetrical about the station line. This allows the inertia matrix to be simplified as

$$I_{XY} = I_{YZ} = I_{XZ} = 0 \quad I_{YY} = I_{ZZ} \quad (3.16)$$

6) The projectile is aerodynamically symmetric.

7) The wind velocity component \hat{u}_w parallel to the projectile station line is negligible in comparison to the projectile total forward velocity.

8) The station line velocity \hat{u} is replaced by the projectile total velocity V as

$$V = \sqrt{\hat{u}^2 + \hat{v}^2 + \hat{w}^2} \approx \hat{u} \quad (3.17)$$

9) The total initial muzzle velocity of the projectile V_o firing sidewise with V_{fir} at an angle ω relative to the helicopter's flight path motion V_{hel} (Figure 3), is

$$V_o = \sqrt{V_{fir}^2 + V_{A/C}^2 + 2 V_{fir} V_{A/C} \cos \omega} \quad (3.18)$$

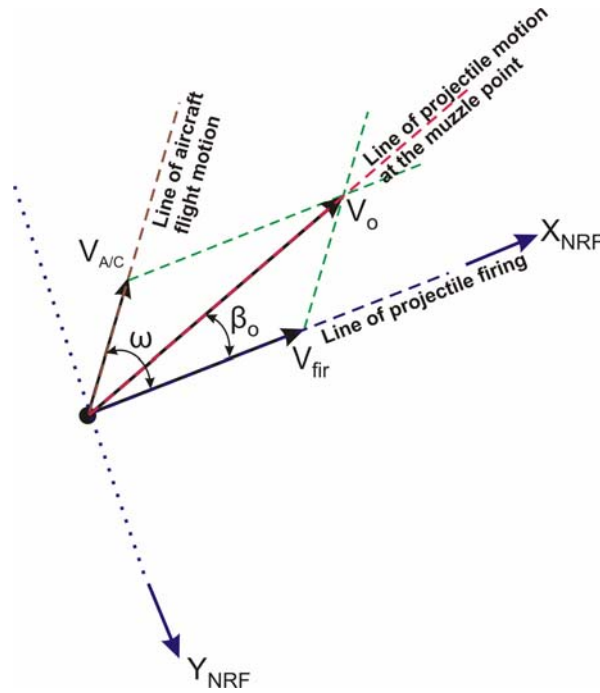


Figure 3: Top view of the initial muzzle velocity at the firing point from M2 automatic gun placed on aircraft's structure

3.1 Initial Spin Rate Estimation

In order to have a statically stable flight projectile trajectory motion, the initial spin rate \hat{p}_o prediction at the gun muzzle in the firing site is very important. According to McCoy (1999) definitions, the following form is used:

$$\hat{p}_o = \frac{2\pi V_o}{\eta D} \quad (\text{rad/s}) \quad (3.18)$$

where V_o is the initial firing velocity (m/s), η the rifling twist rate at the M2 gun muzzle (calibers per turn), and D the reference diameter of the bullet type (m), see Table 1. Typical value of rifling η for the .50 caliber API M8 bullet type is 29.41 cal/turn.

3.2 Aerodynamic Model

For the projectile trajectory analysis, a constant flight dynamic model is proposed for the examined test cases. The above calculations are based on appropriate constant mean values of the experimental average aerodynamic coefficients variations C_D , C_{LA} , C_{MaM} , C_{PD} , C_{OM} and C_{RD} taking from official tabulated database McCoy (1990), as shown in Table 2.

Table 2: Aerodynamic parameters of the applied atmospheric flight dynamic model

Aerodynamic Coefficients	API M8 Bullet
Drag force C_D	0.63
Lift force C_{LA}	3.52
Magnus moment C_{MaM}	0.27
Pitch damping moment C_{PD}	-6.6
Overturning moment C_{OM}	2.6
Roll damping moment C_{RD}	-0.009

4 Angular Oscillatory Motion

The differential equation governing the angular oscillatory motion for the complete linearized pitching and yawing motion of slightly symmetric projectiles as a function of distance traveled s is shown below according to McCoy (1999):

$$\zeta'' + (H - iP)\zeta' - (M + iPT)\zeta = iPG \quad (4.1)$$

where

$$\zeta = \alpha + i\beta \quad (4.2)$$

$$H = \frac{\rho S d}{2m} (C_{La} - C_D - K_y^{-2} C_{PD}) \quad (4.3)$$

$$P = \begin{pmatrix} I_{XX} \\ I_{YY} \end{pmatrix} \begin{pmatrix} pd \\ V \end{pmatrix} \quad (4.4)$$

$$M = K_y^{-2} \left(\frac{\rho S d}{2m} C_{OM} \right) \quad (4.5)$$

$$T = \frac{\rho S d}{2m} (C_{La} + K_x^{-2} C_{MaM}) \quad (4.6)$$

$$G = \frac{gd \cos \phi}{V^2} \quad (4.7)$$

This differential equation contains all the significant aerodynamic forces and moments that affect the pitching and yawing motion of a spinning (or non-spinning) symmetric projectile body. The author's definition $\zeta = \alpha + i\beta$ was first chosen by Fowler et al. Gunners and engineers usually prefer this definition. The gunner observer looks downrange from a position located just behind the gun. Upward and to the right are always considered as positive directions. It is nature for the gunner to define the α axis as positive upward, the β axis as positive to right and the clockwise direction of all rotations as positive for right hand twist rifling.

5 Computational Results

The flight dynamic model of 12.95 mm M8 API (see for example Gkritzapis et. al. 2007; Gkritzapis et. al. 2008) type involves the solution of the set of the twelve nonlinear first order ordinary differential, Eqs (3.2-3.13), which are solved simultaneously by resorting to numerical integration using a 4th order Runge-Kutta method and the solution of the second order differential equation of motion.

Initial flight conditions for the dynamic trajectory bullet model with constant aerodynamic coefficients are illustrated in Table 2, assuming different firing angles $\omega = 30^\circ, 60^\circ$ and 90° with the supersonic firing velocity of $V_{fir} = 900 \text{ m/s}$ relative to the aircraft's high subsonic flight motion of almost $V_{hel} = 230 \text{ m/s}$ (Mach number flight $M = 0.67$).

Table 3: Initial flight parameters of the examined bullet test cases at firing angles $\omega = 30^\circ, 60^\circ, 90^\circ$

Initial Flight Data	API M8 Bullet
Position x , m	0.0
Position y , m	0.0
Position z , m	100.0
Roll angle φ , deg	0.0
Pitch angle θ , deg	0.0
Yaw angle ψ , deg	0.0
Velocity \hat{u} , m/s	900.0
Velocity \hat{v} , m/s	-230
Velocity \hat{w} , m/s	0.0
Roll rate \hat{p} , rad/s	14,830.0
Pitch rate \hat{q} , rad/s	0.0
Yaw rate \hat{r} , rad/s	0.0

The angle of attack α versus angle of sideslip β flight path trajectory motions with the numerical 6-DOF analysis (red color lines) and classical analytical differential equation (green color lines) are indicated in Figure 4a for the 12.95 mm bullet with initial firing velocity of 900 m/s, firing sidewise at 30 deg with

aircraft's velocity 230 m/s. The produced initial yaw (or sideslip) angle is approximately 6 deg. The corresponding initial yaw angle for firing sidewise at 60 deg relative to the aircraft's velocity flight path is approximately 11.2 deg (Figure 4b). Firing sidewise at 90 degrees (perpendicular) of the aircraft's flight path motion gives initial yaw angle at about 14.7 deg, as shown in Figure 4c.

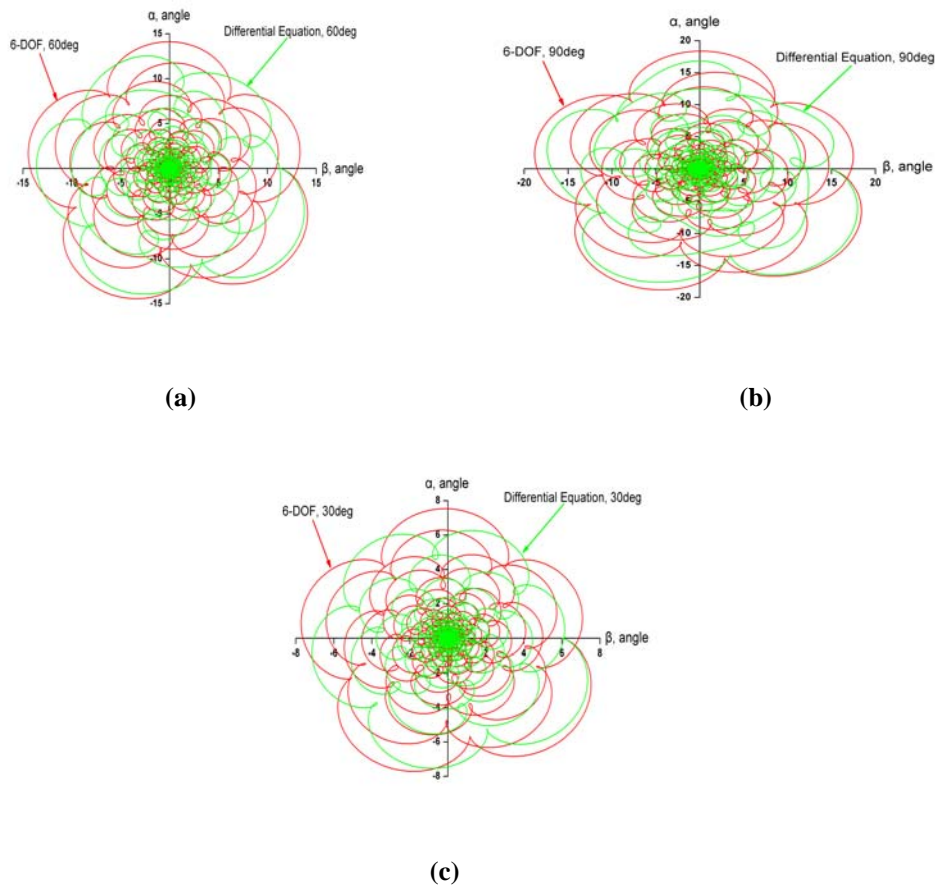
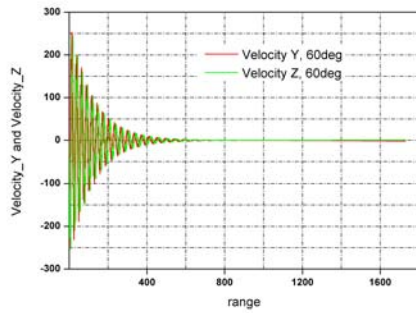
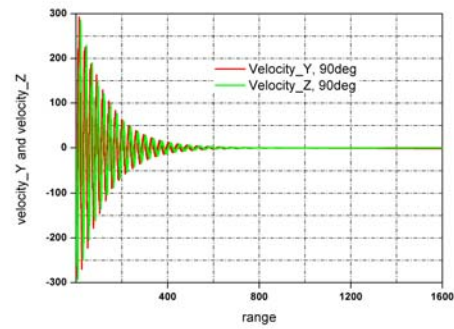


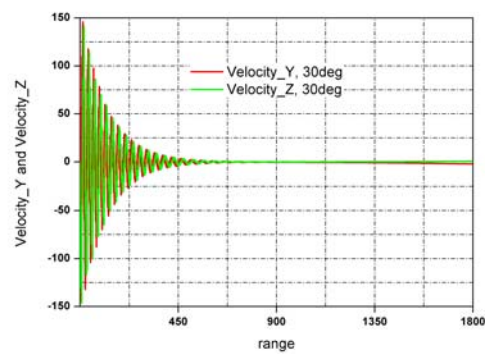
Figure 4: Coupled pitching and yawing motion for the .50 API M8 bullet fired sidewise at different angles ω from a high subsonic air vehicle flying at 230 m/s



(a) 30 deg



(b) 60 deg



(c) 90 deg

Figure 5: Cross velocities in Y and Z directions versus range for the .50 API M8 bullet fired sidewise at different angles ω from a high subsonic air vehicle flying at 230 m/s

The side velocities in Y and Z directions versus range are also investigated for the examined 12.95 mm bullet diameter, using the numerical 6-DOF flight motion analysis firing sidewise from the aircraft's machine gun at angles 30, 60 and 90 deg, as indicated in Figures 5a, 5b and 5c, respectively.

6 Conclusions

The epicyclic pitching and yawing motion of the 6-DOF flight dynamic modelling for flat-fire free flight trajectories is compared with the corresponding classical analysis by using the linear second order differential equation of external motion. The above are applied for the prediction of spin-stabilized projectile trajectories, as the 12.95 mm M8 API bullet projectile type, launched horizontally (from different firing angles) from high-speed subsonic airplanes with constant aerodynamic force and moment coefficients based on official tabulated database for the examined bullet.

References

- [1] M.J. Amoruso, Euler angles and quaternions in six degree of freedom simulations of projectiles, *Technical note*, 1996.
- [2] B. Etkin, *Dynamics of atmospheric flight*, John Wiley and Sons, New York, 1972.
- [3] R.H. Flower, E.G. Gallop, C.N.H. Lock and H.W. Richmond, The aerodynamics of spinning shell, *Philosophical Trans. of the Royal Society of London*, **221**, (1920).
- [4] D.N. Gkritzapis, E.E. Panagiotopoulos, D.P. Margaritis and D.G. Papanikas, Computational atmospheric trajectory simulation analysis of spin-stabilized projectiles and small bullets, *Atmospheric Flight Mechanics Conference and Exhibit*, **AIAA Paper 2007-6584**, Hilton Head, South Carolina, (2007).
- [5] D.N. Gkritzapis, E.E. Panagiotopoulos, D.P. Margaritis and D.G. Papanikas, 2008. Flat-fire aerodynamic jump performance of projectiles fired from a helicopter, *J. of Battlefield Technology, Firepower and Protection*, **11**, (2008), 1-8.

- [6] L.C. Hainz and M. Costello, Modified projectile linear theory for rapid trajectory prediction, *J.of Guidance, Control and Dynamics*, **28**, (2005).
- [7] R. McCoy, The aerodynamic characteristics of .50 Ball, M33, API, M8 and APIT, M20 ammunition, *Ballistic Research Laboratory, Memorandum Report, BRL-MR-3810*, (1990).
- [8] R. McCoy, Modern exterior ballistics, *Schiffer, Attlen, PA*, 1999.
- [9] E.J. Mcshane, J.L. Kelley and F.V. Reno, Exterior ballistics, *University of Denver Press*, 1953.
- [10] T.H. Sterne, The effect of yaw upon aircraft gunfire trajectories, *Ballistic Research Society*, **345**, (1943).

Nomenclature

- a_t : total angle of attack, $a_t = \sqrt{\alpha^2 + \beta^2}$, deg
- C_D : drag force aerodynamic coefficient
- C_{LA} : lift force aerodynamic coefficient
- C_{RD} : roll damping moment aerodynamic coefficient
- C_{PD} : pitch damping moment aerodynamic coefficient
- C_{OM} : overturning moment aerodynamic coefficient
- C_{MaM} : Magnus moment aerodynamic coefficient
- D : projectile reference diameter, m
- g : acceleration gravity, m/s^2
- I_{XX} : projectile axial moment of inertia, $kg \cdot m^2$
- I_{YY} : projectile transverse moment of inertia about y-axis through the center of mass, $kg \cdot m^2$
- I_{XX}, I_{YY}, I_{ZZ} : diagonal components of the inertia matrix
- i : Complex number ($i = \sqrt{-1}$)

K_x^2	: non-dimensional axial moment of inertia, $\frac{I_{xx}}{mD^2}$
K_y^2	: non-dimensional transverse moment of inertia, $\frac{I_{yy}}{mD^2}$
L_{CGCM}	: distance from the center of mass (CG) to the Magnus center of pressure (CM) along the station line, m
L_{CGCP}	: distance from the center of mass (CG) to the aerodynamic center of pressure (CP) along the station line, m
l	: dimensionless arc length
m	: projectile mass, kg
P	: non-dimensional axial spin rate
$\hat{p}, \hat{q}, \hat{r}$: projectile roll, pitch and yaw rates in the moving frame (NRF), respectively, rad/s
t	: time, sec
$\hat{u}, \hat{v}, \hat{w}$: projectile velocity components expressed in the no-roll-frame (NRF), m/s
V	: total aerodynamic velocity, m/s
V_T	: total velocity, m/s
V_o	: total initial firing velocity, m/s
$V_{A/C}$: aircraft's firing velocity, m/s
V_{fir}	: projectile's firing velocity, m/s
S	: projectile reference area ($\pi D^2/4$)
x, y, z	: projectile position coordinates in the inertial frame (if), m

Greek Symbols

α, β	: aerodynamic angles of attack and sideslip, deg
η	: rifling twist rate of the machine gun, calibers/turn
ρ	: density of air, kg/m ³
φ, θ, ψ	: projectile roll, pitch and yaw angles, respectively, deg

